Chemical Cartography: Finding the Keys to the Kinetic Labyrinth

GEORGE W. FLYNN

Very high resolution lasers allow spectroscopic pictures to be taken following a collision between two molecular reactants. The features of these "pictures" are the electronic, vibrational, rotational, and translational motions of the atomic particles, which relate the quantum states of the reactants to the quantum states of the products. Such state-to-state kinetic information can be used to test the shape and nature of the interaction potential that controls the collision process. The potential itself is akin to a map of the terrain through mountains and valleys where elevation is a measure of energy instead of height. Accurate mapping of this potential surface leads to an understanding of the forces which control rates and mechanisms of chemical reactions. The application of four different advanced laser techniques to the study of collisions between "hot" hydrogen (H) atoms and carbon dioxide (CO_2) molecules has provided a wealth of information about both reactive and nonreactive collisions for this system. The availability of data for rotationally, vibrationally, and translationally inelastic excitation of CO_2 by H atoms, when compared with data for reactive events producing OH + CO, provides insights into the dynamics of collisions between H and CO_2, and illustrates the future promise of these powerful techniques for elucidating features of potential energy surfaces.

CHEMICAL REACTIONS CERTAINLY INFLUENCE OUR LIVES. Not only are they critical in determining the "health" of our atmosphere, they also control the very processes of life within the bodies of all living things. There are basically two aspects of individual chemical reactions that determine their relative importance. The first is the equilibrium point of the reaction, and the second is the rate at which the reaction occurs at a given temperature. In the first half of this century, thermodynamic measurements were refined sufficiently to provide the necessary reaction parameters, enthalpy ΔH and entropy ΔS, to predict the equilibrium point for a large number of important chemical reactions.

Rates of chemical reactions have also been studied for some time with a variety of techniques. Most of the early studies focused on the bulk reaction rate by which large quantities of material reacted to form new products. For example, the reaction of hydrogen atoms with carbon dioxide to form hydroxyl radical and carbon monoxide can be written

$$H + CO_2 \rightarrow OH + CO$$

The simplest characterization of the rate for a chemical reaction of this kind is the kinetic rate law, which for the above reaction might be written

$$-d[H]/dt = d[CO]/dt = k[H][CO_2]$$

where k is the rate constant, t is time, and brackets indicate concentrations in moles per liter or number of molecules per cubic centimeter.

This rate law represents an immense oversimplification of the kinetic process because, thanks to the advent of modern quantum theory, we recognize that the reactants and products are actually composed of a large number of molecules with very different properties. These properties are the electronic, vibrational, rotational, and translational energies of the individual molecules. Classical reaction rate studies only tell us how the average H reacts with the average CO_2 to produce the average OH and CO. Modern efforts aimed at the study of chemical reaction rates focus on the quantum nature of matter and at least attempt to ask which of the initial states of the reactants lead to which final states of the product. Or, said another way, what is the probability that an individual quantum state in the reactants will lead to a particular quantum state of the products? The possibility of asking this question, despite the obvious complexity of the reaction process which involves many different quantum states, is due to several developments in the field of chemical dynamics that have occurred during the past 35 years but particularly in the past decade. These developments are the perfection of high-vacuum techniques, the invention and commercial availability of lasers, the discovery of supersonic expansion methods for cooling molecules in the gas phase to a few kelvins, and the dramatic increase in computing power that has made the theoretical investigation of these quantum state–resolved scattering processes feasible. All of these developments have given rise to the field of "state-to-state kinetics." Investigations in this field are leading to fundamental insights into the nature of chemical reactions, in some cases confirming many of the old "pictorial" ideas about kinetic processes and in some cases contradicting such simple pictures but providing new physical insights.

The availability of very high resolution lasers ($0.0003\ cm^{-1}$) literally allows a spectroscopic "snapshot" to be taken following a kinetic encounter between two molecular species. The topological features of these snapshots are the electronic, vibrational, rotational, and translational motions of the atomic particles. Why is this added detail of interest, particularly since substantial experimental effort is

---

The author is in the Department of Chemistry and Columbia Radiation Laboratory, Columbia University, New York, NY 10027.

required to obtain this kind of kinetic information? The key reason is that such data can be used to test the shape and nature of the interaction potential that controls the collision dynamics. The potential itself is like a map of the mountains and valleys of a rugged terrain, except that the heights of the hills are measured in units of energy rather than elevation. The task then is to make a map of the potential energy surface by studying the labyrinth of pathways leading from the many quantum states of the reactants through the energy mountains of the surface to the quantum state valleys of the final products. The study of quantum state–resolved (state-to-state) collision dynamics simply provides a high-resolution picture that can be used to sense the mountainous terrain between reactants and products. Once the potential "surface" has been accurately mapped, most of the features of a chemical reaction or a collisional encounter can be predicted, thus leading to a complete understanding of the forces that control the rate and mechanism of a chemical reaction.

The $H^* + CO_2$ Collision Process

To illustrate the remarkable advances in the area of state-to-state collision dynamics, consider the collisional encounter between fast-moving H atoms and CO_2 to produce two different sets of final products

$$H^* + CO_2 \rightarrow OH + CO$$

$$H^* + CO_2 \rightarrow H + CO_2\#$$

where H^* is a hydrogen atom with very high translational energy, generally called a "hot" atom, and $CO_2\#$ is an excited CO_2 molecule. The existence of two different sets of "products" illustrates an extremely important feature of the collision dynamics between a hot H atom and a CO_2 molecule. One must remember that not all collisional encounters lead to chemical reaction. In fact, for most H^*-CO_2 interactions, "quenching" of the H^* atom without chemical reaction, leading to vibrationally, rotationally, and translationally excited $CO_2\#$, is more common than reaction to form the new, chemically distinct products OH and CO.

The reaction process leading to OH + CO is, nevertheless, an extremely interesting one. The reverse reaction in which OH combines with CO to form H + CO_2 has been called the second most important reaction in the combustion field (*1*), and it plays a significant role in atmospheric science as well (*2*). The collisional encounter between H and CO_2 is of particular interest because four of the most powerful and elegant experimental techniques available at present for studying chemical dynamics have been applied to this system, and because extensive, advanced theoretical studies have been performed to investigate the features of the H^*-CO_2 potential energy surface that control the collision dynamics for this encounter. The combination of these experimental and theoretical efforts has led to remarkable insights into the nature of the collision process between these two species.

Studies of the $H^* + CO_2$ reaction system date back to the 1960s when hot hydrogen atoms were produced by photolyzing HI with ultraviolet (UV) light in the presence of CO_2 (*3*). Reaction products were analyzed with gas chromatography and a threshold energy was determined. No information about nonreactive encounters and relatively little data about the microscopic dynamics could be obtained from these experiments because the time scale was the order of hours, too long to resolve individual collision events, of course. In 1981 the study of hot atom collisions was reinvigorated when the first laser experiments were performed with short pulse excimer lasers to produce hot atoms (*4*).

$$H_2S + h\nu(193\text{ nm, }20\text{ ns}) \rightarrow H^*(230\text{ kJ/mole}) + HS$$

where h is Planck's constant and ν is the frequency of the light.

The excimer laser, operating at a single UV wavelength of 193 nm and at very high power, can produce large quantities of very fast moving H atoms that are largely monoenergetic. The short (20-ns) pulse nature of these devices means that the hot atoms are made on a time scale that is very short compared to molecular collisions for samples at a pressure below 1.0 torr. All of the techniques described below take advantage of this short pulse nature of the H^* production to follow the subsequent collision dynamics of the atoms with fast transient experimental hardware. These fast analysis methods allow the effects of only the first collision between H^* and CO_2 to be followed in real time (20 ns).

The four techniques that have been used most successfully to follow the collision dynamics of the $H^* + CO_2$ interaction are: (i) infrared (IR) diode laser probes of the nonreactive, but vibrationally, rotationally, and translationally inelastic excitation of CO_2; (ii) UV laser probes of the bulk gas (0.05 torr) chemical reaction producing OH + CO; (iii) UV laser probes of photoinduced reactions of van der Waals complexes made by supersonic expansion, such as $HBr \cdot CO_2$, to produce OH + CO; and (iv) real time (picosecond) monitoring of the breakup of the $HI \cdot CO_2$ van der Waals complex to produce OH + CO. Taken together, these experimental techniques provide an astonishing amount of information about collisions that produce reaction or just vibrational, rotational, and translational excitation of the $CO_2\#$ product. The results of these experiments are briefly reviewed below.

Inelastic Excitation of CO_2 by Hot H Atoms

The experiments designed to monitor quantum-state–resolved, nonreactive energy changes in CO_2 caused by H^*-CO_2 collisions made use of IR diode laser absorption spectroscopy to probe the CO_2 (*5–15*). They can be summarized by the following equations that describe H^* production, collisional excitation, and laser probing, respectively

$$H_2S + h\nu(193\text{ nm, }20\text{ ns}) \rightarrow H^*(230\text{ kJ/mole}) + HS$$

$$H^* + CO_2(00^00, J', V') \rightarrow H + CO_2(mn^lp, J, V)$$

$$CO_2(mn^lp, J, V) + h\nu(4.3\ \mu m) \rightarrow CO_2\ (mn^lp + 1, J + 1,\ V)$$

Here m, n, and p are the quantum numbers for the CO_2 vibrational modes ν_1 (1337 cm^{-1} or 16.0 kJ/mole), ν_2 (667 cm^{-1} or 8.0 kJ/mole), and ν_3 (2349 cm^{-1} or 28.1 kJ/mole), respectively, J and l are the rotational and vibrational angular momentum, respectively, and V is the CO_2 velocity whose mean value after the collision can be determined by measuring the transient Doppler broadening of the CO_2 IR transitions (*13*). This kind of measurement is only possible because of the extraordinary resolution of the IR diode laser. A physical picture of the CO_2 normal modes is shown in Fig. 1. The source of the 4.3-μm IR light is a diode laser that is continuously tunable (over a range of 50 to 150 cm^{-1}) and spectrally pure (<0.0003 cm^{-1} linewidth).

In these experiments CO_2 molecules start out in the ground, or zero-point vibrational level, $CO_2(00^00)$, with a thermal distribution of angular momentum quantum states J' and velocities V'. Collisions with H^* then produce a host of final vibrational and rotational levels, each with its own recoil velocity profile V. Rotational and vibrational state population distributions, as well as velocity distributions, resulting from H^*-CO_2 collisions have been measured for the 00^01 antisymmetric stretching fundamental level (*5, 7, 9, 11, 13, 15, 16*), the 10^00 symmetric stretching fundamental level (*17*), the

01^11 bend-stretch combination level (*18*), and the 00^02 antisymmetric stretch "overtone" level. Partial rotational distributions are also available for other vibrational states. An intriguing feature of these experiments is the expectation that the different vibrational modes, reflecting as they do different atomic motions of the CO_2 molecule (see Fig. 1), act as indicators of the relative efficiencies of "end-on" versus "broadside" collisions in producing translational, rotational, and vibrational excitation of the molecule. End-on collisions are those in which the H atom strikes the CO_2 molecule near the O atom moving in a direction parallel to the molecular axis, whereas broadside collisions are those in which the H atom strikes the CO_2 molecule near the C atom moving perpendicular to the molecular axis. This expectation has been at least qualitatively borne out in the data obtained so far, although more precise theoretical computations are required before quantitative comparisons between the experimental data and these simple ideas are possible.

To illustrate the kind of data obtained from these experiments, consider collisions that excite the antisymmetric stretching vibrational state 00^01 (*9, 11, 13, 15, 16*). The rotational population distribution for this state produced by H* collisions peaks at about $J = 39$, well above the most probable room-temperature thermal value of $J' = 16$ in which the molecules started. Typical changes in angular momentum ΔJ correspond to 30 to 40 units of $h/2\pi$, and the falloff in population for $J > 39$ is almost certainly due to the conservation of angular momentum. A simple calculation shows that J values up to 200 are allowed based on energy constraints, but that the total angular momentum available in the collision (orbital angular momentum of the H*-CO_2 collision plus initial angular momentum J' of the CO_2 00^00) limit the final J to the range from 0 to 75. In fact, the maximum J value is actually limited by the molecular dimensions of CO_2, since the orbital angular momentum in a collision is $L = \mu v b$, where μ is the reduced mass of the H-CO_2 complex, v is the velocity of the H atom, and b is approximately the distance of closest approach of H to CO_2 during a collision that produces excitation. The maximum value of b, which determines the maximum value of L since μ and v are fixed in these experiments, is set by the dimensions of the CO_2 molecule to be ~2 Å. This results in a maximum L of about 50 times $h/2\pi$. For initially nonrotating CO_2 molecules, the final angular momentum J cannot exceed L. Somewhat larger J values can result from collisions between initially rotating CO_2 molecules and H atoms.

The average translational recoil energy ΔE of the CO_2 in this state is given by a remarkably simple formula that treats the H*-CO_2 collision as an impact between two billiard balls (*13, 19*).

$$\Delta E = [2M_HM_{CO_2}/(M_H + M_{CO_2})^2]E_a$$

where E_a is the energy available for translation (the collision energy less the energy going into vibration and rotation) and M_I is the mass of species I. Despite this simple average result for the 00^01 state, there is a subtle but quite clear increase of ΔE with increasing J within the 00^01 rotational state. This result shows that the high J levels of 00^01 are produced by the most direct, "hard" collisions, whereas the lower rotational levels are produced by at least somewhat more glancing, "softer" collisions (*16*).

The detailed data that are now available suggest that simple physical insights can provide some reliable predictions for inelastic scattering in this system, but extensive calculations with excellent potential energy surfaces are required to test the concepts developed here. Data of this type serve as a most rigorous test for the quality of calculated potential energy surfaces. Indeed, surfaces for H* + CO_2 seem to be quite successful in predicting the reactive properties of the system as noted below, but they are much less successful in forecasting the vibrationally, rotationally, and translationally inelastic scattering data (*20*).

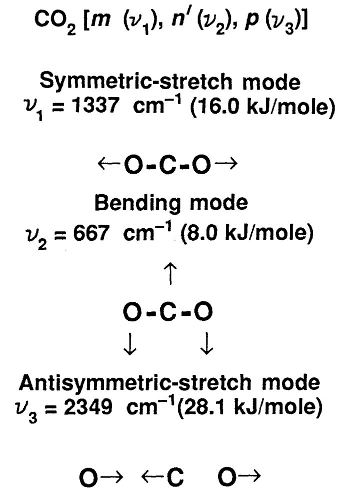

Fig. 1. The physical motions of vibrating CO_2 molecules are shown, where ν_1 is the symmetric stretching motion, ν_2 is the bending motion, and ν_3 is the antisymmetric stretching motion. Each vibrational motion or mode behaves approximately like an independent harmonic oscillator: $m = 0, 1, \ldots$ is the quantum number for ν_1; $n = 0, 1, \ldots$ is the quantum number for ν_2; $p = 0, 1, \ldots$ is the quantum number for ν_3; and l is the vibrational angular momentum associated with the bending motion.

Chemical Reaction of Hot H Atoms with CO_2

All three of the different types of experiments probing the reactive channel for the H* + CO_2 interaction make use of the same basic laser technique for product analysis. The experiments can be summarized by the following chemical equations that describe reaction, laser excitation, and fluorescence detection, respectively:

$$H^*(^2S) + CO_2(X^1\Sigma) \rightarrow HCO_2^* \rightarrow OH(X^2\Pi,v,N) + CO(X^1\Sigma,v',J)$$

$$OH(X^2\Pi,v,N) + h\nu(306 \text{ to } 315 \text{ nm}) \rightarrow OH(A^2\Sigma,v,N')$$

$$OH(A^2\Sigma,v,N') \rightarrow OH(X^2\Pi) + h\nu'(\lambda > 320 \text{ nm})$$

Here v labels vibrational quantum numbers of the two diatomic species OH and CO, N is the angular-momentum quantum number for OH (composed of both electronic and overall rotational angular momentum), and J is the overall rotational angular momentum of the CO product. HCO_2^* is an "intermediate complex" of high energy through which the reaction is presumed to proceed. Although this complex may be usefully thought of as the reaction transition state, it does not fit the strict definition of a transition state (the maximum energy point on the lowest energy path from reactants to products) in all experiments.

The detection scheme used here is the extremely powerful and versatile "laser-induced fluorescence" (LIF) method, invented in the early 1970s (*21*). The basic idea is to use a short pulse (typically 10 to 20 ns), frequency-tunable, high-resolution laser (such as one operating at 310 nm) to probe very specific quantum states of the product $OH(X^2\Pi,v,N)$ by exciting only the particular molecules in the v,N level to an electronically excited state. After proper normalization, the fluorescence emitted from the excited electronic state is proportional to the number of molecules initially formed in the $OH(X^2\Pi,v,N)$ state by the chemical reaction. Since no monochromator is required and the laser can be focused to a small, intense spot, exceedingly high sensitivity is possible with such a probe technique.

The short pulse nature of the laser allows excellent time resolution in the experiments so that collisions occurring subsequent to $OH(X^2\Pi,v,N)$ formation do not "scramble" the initial distribution produced by the reaction. The frequency tunability simply allows, within rather broad limits, any v,N state to be probed. Finally, the Doppler profile of the OH product can also be determined to provide information about its translational recoil. These studies also require a short burst of H* atoms to maintain good time resolution, but this is easily accomplished by UV photolysis of HBr, HI, or H_2S, as described above for the vibrationally, rotationally, and translationally inelastic H* + CO_2 studies. Although in all of the experiments the same detection technique is used, several clever variants on sample preparation and pulse timing have been used to obtain remarkably detailed, fascinating information about the same extremely important and interesting reaction. The three types of experiments are considered separately below.

Bulk gas phase studies of H + CO_2.* The first and experimentally simplest study of the reaction between hot H* atoms and CO_2 was carried out with low-pressure, room-temperature samples of CO_2 and an H atom precursor such as H_2S or HBr (*22–25*). These experiments are completely analogous to the vibrationally inelastic collision studies described above. The differences are that the reactive channel that produced OH + CO was monitored rather than the nonreactive channel that produced H + CO_2; LIF was used to probe the final quantum states of the OH($X^2\Pi$,v,N) product as described above. As in the vibrationally inelastic collision studies, all collision geometries between the H* and CO_2 are sampled in these types of experiments because collision trajectories are random in low-pressure gas-phase samples. Many studies of the reaction of H* and CO_2 have now been reported (*22–25*), the most recent of which is an investigation of the energy dependence of this process where tunable lasers were used to photolyze the precursor HI, producing H* atoms with varied energy (*24*).

The reaction produces mostly v = 0 OH but the rotational distribution of the radical diatomic fragment is peaked at N values of about 6 to 8 for a collision energy of 227 kJ/mole. The v = 1 OH product accounts for only 10% of the total cross section, which is 0.4 ± 0.2 Å^2 at a collision energy of 179.5 kJ/mole (*25*). The small cross section is in itself quite surprising, since the hot atom collision energy is well above the reaction energy barrier of 111.3 kJ/mole. The reaction cross section falls to < 0.003 Å^2 at an energy of 123.1 kJ/mole (*23, 24*). The rotational energy distributions of the OH product become less broad as the H* + CO_2 collision energy decreases, and the peak rotational state falls from N values of 6 to 8 near 227 kJ/mole to values of 2 to 3 at collision energies of 123.1 kJ/mole (*23, 24*). Unfortunately, quantum state–resolved studies of the CO(v,J) product are just beginning (*26*).

High-resolution probing of the breakup of supersonically prepared HCO_2 complexes: Vibrational and rotational OH product distributions.* The first studies of the chemical reaction of van der Waals complexes were performed with HBr · CO_2 precursors prepared by standard supersonic expansion methods resulting in gas-phase samples of this complex that can be characterized by a temperature of the order of a few kelvins (*27*). Excimer lasers operating at 193 nm were used to photodissociate the HBr moiety in the complex, producing high-energy H atoms that then "collide" with CO_2, reacting to form OH + CO. The OH($X^2\Pi$,v,N) product distributions were then probed with the use of relatively long (10-ns) laser pulses (310 nm). Recent experiments have extended the technique to measuring the OH product from HI · CO_2 complexes that were photodissociated with tunable lasers (λ from 233 to 263 nm) to provide reaction complexes of different energy (*23, 24*). The idea of these experiments is to prepare HOCO complexes with a restricted geometry in the hope of obtaining information about the reaction pathways for specific geometries of the "transition state complex." Since the van der Waals complex has a relatively well-defined geometry and the photodissociation process takes place on a time scale that is short compared to the motions of the atoms, the reaction can be reasonably presumed to proceed along a path set by the initial shape of the van der Waals complex.

The OH rotational state population distributions for the supersonically prepared samples peaked at lower energies than the bulk phase reaction of the same type, in which reaction geometry is unrestricted since collisions between H* and CO_2 are allowed from all directions. The cooler rotational distributions have been attributed to a trapping of the H atom between the heavy Br and CO_2 fragments. Thus the light atom behaves somewhat like a particle in a box that slowly expands as the Br and OCO fragments separate from each other. As the H atom "rattles" back and forth in its box or cage, it imparts kinetic energy to the separating Br and CO_2 fragments and thus leaves less internal (rotational and vibrational) energy for the HOCO* product (*23, 24, 28, 29*). Since no such trapping effect occurs in bulk phase reactions where Br and CO_2 are always well separated, the HOCO* complexes formed in the bulk phase tend on average to have more available energy to impart to the product OH resulting in hotter rotational energy distributions.

Picosecond time-resolved probing of the breakup of supersonically prepared HCO_2 complexes.* The newest of the experimental techniques used to study the H* + CO_2 reaction is perhaps the simplest to conceptualize. In these experiments, HI · CO_2 van der Waals complexes prepared as described above by standard supersonic expansion techniques result in gas phase samples of this complex that can be characterized by a temperature of the order of a few kelvins. A picosecond photodissociating pulse (239 nm), derived with the use of standard nonlinear laser-mixing techniques, was used to "remove" I atoms from the complex by photodissociating the HI chromophore to leave high-energy "HOCO." The HOCO then dissociates to form OH + CO. The OH product was then probed, by LIF as described above with a second picosecond laser (308 nm) delayed by varying times (0 to 30 ps) from the first photolyzing pulse. In this way the actual birth of the OH from the HOCO complex could be followed.

The one new piece of information obtained from this study is the buildup time of the OH radical species, 5 ± 2 ps, which is assumed to be the same as the breakup time for the HOCO complex. Note that the HOCO complex is of very high energy because it "contains" the kinetic energy of the hot H atom resulting from the photolysis of HI in the van der Waals complex. This energy is either 200 kJ/mole or 112 kJ/mole depending on whether the I atom leaves the complex in its ground or excited electronic spin state. Since the reaction has a minimum energy barrier of about 111 kJ/mole (see Fig. 2), both of these channels could in principle contribute to the observed breakup

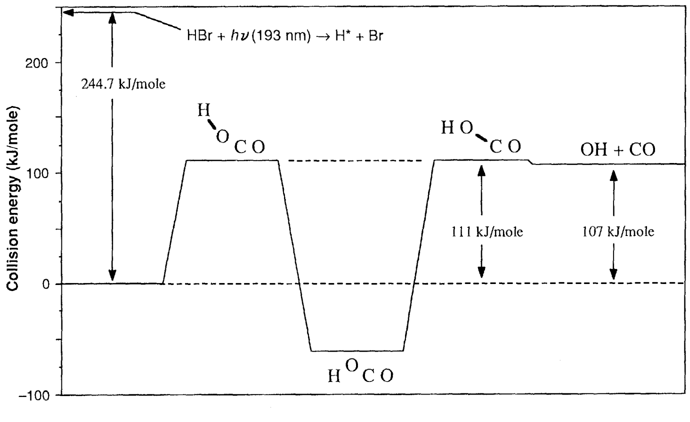

Fig. 2. Shown is a simplified energy diagram for the various species of importance in collisions between hot hydrogen atoms and CO_2 to form OH + CO. The most stable species on the minimum energy path from reactants to products is *trans*-HOCO (slightly more stable than the cis form, which is not shown in the diagram) from which reaction to form products occurs. Isomerization from *cis*-HOCO to *trans*-HOCO is facile (low, 34-kJ/mole barrier). The overall barrier for the reaction is 111 kJ/mole, well below the initial collision energy of 244.7 kJ/mole typical of encounters between hot H atoms and CO_2. The highest frequency vibrational mode of CO_2 (see Fig. 1) has an energy of 28.1 kJ/mole. Note that the initial approach of H to CO_2 is everywhere repulsive.

of the HOCO complex; however, given the sharp drop-off in reaction probability with "collision" energy noted above (*23, 24*) for the bulk phase reaction, contributions from the 112 kJ/mole channel are most likely negligible compared with the 200 kJ/mole channel.

Ideally, these experiments can be viewed as the preparation of a high-energy HOCO complex by photodissociation of the $HI \cdot CO_2$ van der Waals species, followed by the breakup of the complex to form the chemical products OH + CO. In fact, these events are not totally separated, because the departing I atom is still in the vicinity of the HOCO when breakup begins. As noted above, this can lead to the "trading" of available reaction energy for I atom and CO_2 kinetic energy (*23, 24, 28, 29*). Note also that the spectral information contained in the $OH(X^2\Pi,v,N)$ quantum states is largely lost in these experiments because the short duration of the probing laser pulse limits the laser frequency resolution to about 10 cm^{-1}. Nevertheless, these elegant experiments provide an intriguing piece of information that must be fit together with the other pieces of the $H^* + CO_2$ puzzle to obtain a unified picture of the dynamics.

Comparison of Theoretical Calculations with Experimental Data

In comparing the available data with relevant theoretical calculations for the reactive $H^* + CO_2$ system, the one-dimensional energy diagram shown in Fig. 2 is useful. The HOCO′ complex has several stable isomers (*20*). These are the trans form shown in Fig. 2, in which H and O′ are opposite each other across the CO bond; the cis form (not shown in Fig. 2), in which H and O′ are on the same side of the CO bond; and HCO_2, in which the H is attached to the carbon. A three-dimensional representation of the potential energy surface for the $H + CO_2$ collisional interaction is shown in Fig. 3. The view in this picture is broadside to the O-O axis of CO_2 looking at the C atom in the center. This potential energy surface was calculated by fixing the position of the H atom with respect to the CO_2 center of mass, allowing the CO_2 to bend and stretch, and then minimizing the energy with respect to the CO_2 geometry (*20*). Thus the surface represents the bent cis, trans, and H-CO_2 complexes as well as can be obtained with the present theoretical state of the art.

The H-CO_2 interaction is highly repulsive (an energy of at least 110 kJ/mole) everywhere (the "foothills" before the tall mountains) except along a line perpendicular to the OCO axis at the C atom. Here there is a small plateau with an energy of 54 kJ/mole, and beyond this a well or valley corresponding to stable H-CO_2 where H is attached to the C atom. Movement from the H-CO_2 well to the wells for *cis-* and *trans*-HOCO is severely restricted by a high-energy barrier (138 kJ/mole). Thus isomerization of HCO_2 to *cis-* or *trans*-HOCO is not facile on this surface. Reaction to form OH + CO takes place from the trans configuration, which can proceed to products with no exit-channel barrier. The minimum reaction path leading from $H^* + CO_2$ to OH + CO requires formation of *cis*-HOCO and isomerization to *trans*-HOCO followed by reaction (*20*). This isomerization step is facile (with a barrier of only 34 kJ/mole), so that once *cis*-HOCO has been formed, reaction proceeds readily.

The optimum geometry for stable *cis*-HOCO requires the OCO bond to be bent away from a linear geometry by an angle of approximately 21°, whereas CO_2 itself is linear. Since the fluctuations for the CO_2 zero-point bending-vibration angle are only about 7°, collisions between fast H atoms and linear CO_2 are very unlikely to be in an optimum geometry for forming the *cis*-HOCO complex (*20*). The short duration of such collisions implies that the heavy OCO "backbone" does not have sufficient time to reorient (bend) under the influence of the H atom in order to form a stable cis complex during most collisions (*23, 24, 28, 29*). This slow response of the OCO frame is believed to account for the rather low reaction cross section for the bulk gas reaction (roughly 1% gas kinetic), despite the available collision energy being well above the reaction barrier. Such a picture makes the connection between the vibrationally inelastic and reactive collision studies remarkably clear, since the bending and stretching of the OCO backbone corresponds to vibrational excitation by the H^*-CO_2 collision process. The increase in reaction cross section with increasing collision energy can be attributed, at least in part, to the increased probability of exciting high-energy vibrational states of CO_2. These highly excited vibrational states, of course, correspond to bent and stretched CO_2, just the geometry changes needed to trap the H atom in the HOCO complex.

Essentially 100% of all reactive encounters between H^* and CO_2 in the bulk phase are found, theoretically, to proceed through a short-lived complex. These same calculations reproduce the OH rotational distributions, the vibrational distributions, and the reaction cross sections quite well (*20*). This result provides strong encouragement that those features of the H^*-CO_2 potential energy surface that determine the reaction rate and the channels leading to the final product quantum states are now known with reasonable accuracy.

Calculations of reaction probability and product state distributions can also be performed without a knowledge of the complete potential energy surface by using transition state theory. Such calculations assume that the reaction proceeds through a transition state complex, and that the final product energy distributions can be determined from the properties of the transition state with statistical methods. The advantage of this approach is that only the properties

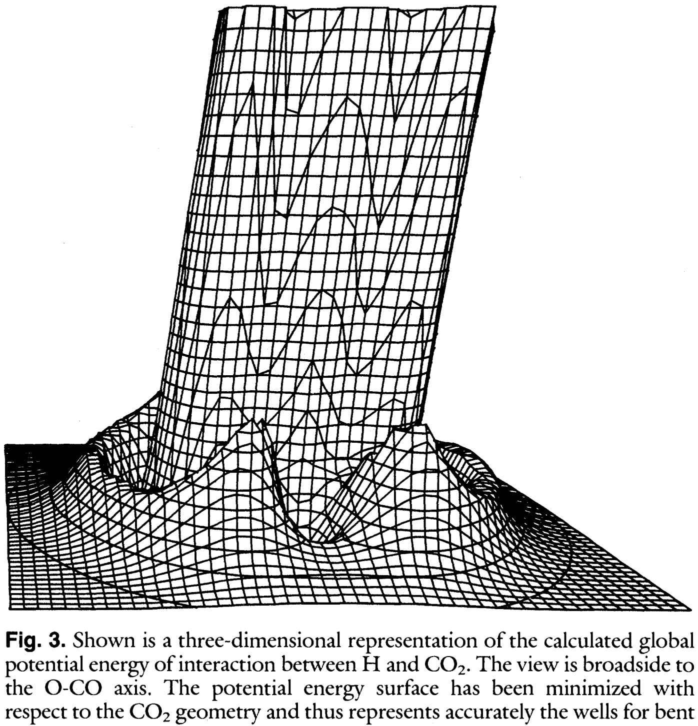

Fig. 3. Shown is a three-dimensional representation of the calculated global potential energy of interaction between H and CO_2. The view is broadside to the O-CO axis. The potential energy surface has been minimized with respect to the CO_2 geometry and thus represents accurately the wells for bent cis, trans, and H-CO_2 complexes. The central plateau (energy, 54 kJ/mole) corresponds to a relative minimum in the repulsion between H and CO_2, beyond which is the well for the stable HCO_2 isomer with H attached to C. Note that the potential seen by H approaching CO_2 is everywhere very repulsive initially (with an energy of at least 110 kJ/mole, see Fig. 2), except at the HCO_2 plateau. Beyond these initial repulsive "foothills" lie the valleys or wells corresponding to "stable" *cis-* and *trans*-HOCO, and beyond these lie the high repulsive mountains corresponding to nuclear core repulsions between H and O or C. [Figure courtesy of G. Schatz]

of the transition state (vibrational frequencies, moments of inertia, and so forth) need to be calculated, rather than the complete potential energy surface. Furthermore, refined transition-state parameters are available for the H* + CO_2 reaction (*31*). The experimental data indicate that, at high collision energy, the product channel translational energy is too large and the rotational energy too small to fit such a statistical calculation, indicating that the reaction is not fully statistical (*23, 24*).

Apparently, the HOCO complex retains some memory of its initial formation, perhaps because the light H atom moves so quickly (0.2 Å/fs) that the initially linear OCO heavy atom group cannot fully sample all possible configurations of the transition state before the complex falls apart to give products. As might be expected, at lower collision energies where the H atom is moving more slowly, the experimental data comes closer to the predictions of statistical theory (*23, 24*).

Theoretical calculations indicate that vibrationally inelastic scattering in the bulk phase generally does not proceed through an HOCO complex. An exception to this is the observation that high-energy vibrational levels are formed at least some of the time through a complex (*20*). Since these high levels have not yet been probed in vibrationally inelastic scattering experiments, complex formation is not likely to play an important role in these studies, assuming that the calculations are correct. The theoretical calculations do indicate that different vibrational modes of CO_2 are excited by different kinds of H*-CO_2 collisions. Thus, end-on encounters are predicted to have a higher probability of exciting antisymmetric-stretching vibration than would broadside collisions (*20*). This result is encouraging for two reasons. First, the data seem to indicate that different modes do show different rotational distributions, which would be expected if, in agreement with theory, different approach geometries were responsible for exciting different modes. Second, rotational population and velocity recoil profiles from different modes should provide tests for different parts of the potential energy surface. This kind of data should substantially improve our ability to correct and refine potential surfaces by comparing data from different modes with calculations based on an assumed potential energy surface.

Theoretical calculations are less well developed for the reactions that begin with an HI · CO_2 or HBr · CO_2 van der Waals complex. Potential surface calculations for the HBr · CO_2 system do not reproduce the OH rotational distributions as well as the calculations for the bulk phase H* + CO_2 reaction (*32*). In addition, the lifetime of the HOCO complex, measured in the picosecond HI · CO_2 photodissociation experiments as 5 ± 2 ps, is calculated to be substantially shorter for the HBr · CO_2 complex. Perhaps one explanation for this is that the actual structure of the HI · CO_2 complex is not yet known. Until recently, all HX · CO_2 complexes were assumed to be linear based on the known shape of the analogous HF (*33*) and HCl (*34*) van der Waals complexes. Recent data for HBr · CO_2 suggests that this moiety is in fact T-shaped with the Br atom perpendicular to the OCO axis (*35*). This difference indicates that the HI · CO_2 structure should not be taken for granted at this time.

Comparisons between the experimental data and statistical calculations (transition state theory) suggest that the breakup of HOCO complexes formed from HBr · CO_2 van der Waals precursor complexes occurs at a lower energy than for the breakup of HOCO complexes formed in the bulk phase. The explanation for this is that the H atom, initially formed by photodissociation, is trapped between the heavy OCO and Br species and transfers some of its initial kinetic energy to translational center of mass energy rather than to the HOCO internal degrees of freedom (*29*). The trapping of the H atom between the heavy species also gives the OCO more time to bend into position to trap the H atom in the *cis*-HOCO configuration. This result would suggest that the reaction cross section for the precursor geometry–limited (PGL) reactions should be greater than the bulk phase cross sections. At present there are no measurements of the PGL cross sections for any reaction. Although the van der Waals complex reactive experiments were conceived to simplify and define the geometry of the "transition state," they have added a new dimension to the understanding of complex reactions by revealing the importance of these dynamical effects.

The statistical calculations also predict too short a lifetime for the HOCO complex (*29*) compared with that observed in the picosecond experiments. The measured lifetime is certainly more characteristic of that expected for a long-lived complex breakup, since the typical vibrational period for the HOCO complex should be in the range of 0.03 ps, much shorter than the measured lifetime of 5 ± 2 ps (*30*). Thus, the HOCO complex from HI · CO_2 appears to exist for typically 100 vibrational periods before decomposition, and this should be more than sufficient to randomize the energy, providing good agreement with statistical calculations. Long lifetimes, of course, do not guarantee statistical behavior in the breakup of a complex such as H-CO_2. Only when all possible quantum states of the system (consistent with the overall energy of the complex) are "sampled" during this lifetime is true statistical behavior expected and observed. Nevertheless, the lack of agreement between the lifetime data and the statistical calculations, taken together with the quantum state–resolved experimental data which also seems to be nonstatistical, remains as one of the intriguing puzzles of this remarkably rich system.

Conclusions

Taken together, these studies present an astonishingly detailed picture of the collision dynamics for the H + CO_2 reaction. When compared with the initial classical experiments, which provided only energy threshold data and approximate cross sections, they show the dramatic advances in chemical kinetics that have been brought about by laser techniques in just the past 8 years. The availability of data for rotationally, vibrationally, and translationally inelastic scattering channels, which compete with the reactive events, adds a degree of insight hitherto unavailable in the field of collision dynamics for atom-polyatomic molecule encounters. It is perhaps not too much to expect that the H* + CO_2 system may, in the near future, become the first fully characterized four atom kinetic system in which precise comparisons between theory and experiment will be the norm rather than the exception. Laser probes are thus providing chemical cartographers with the keys to the labyrinth of possible kinetic pathways that lead from initial reactant quantum states to final product quantum states. The results seem certain to deepen our understanding of chemical reaction mechanisms and ultimately to improve our control of the rates and products of chemical reaction processes.

REFERENCES AND NOTES

1. J. A. Miller and G. A. Fisk, *Chem. Eng. News* **65** (no. 35), 22 (1987).
2. P. M. Banks and G. Kockarts, *Aeronomy* (Academic Press, New York, 1973), p. 362; I. Smith and R. Zellner, *J. Chem. Soc. Faraday Trans. II* **69**, 1617 (1973), and references cited therein.
3. G. A. Oldershaw and D. A. Porter, *Nature* **223**, 490 (1969).
4. C. R. Quick, Jr., R. E. Weston, Jr., G. W. Flynn, *Chem. Phys. Lett.* **83**, 15 (1981); F. Magnotta, D. J. Nesbitt, S. R. Leone, *ibid.*, p. 21.
5. J. O. Chu, C. F. Wood, G. W. Flynn, R. E. Weston, Jr., *J. Chem. Phys.* **80**, 1703 (1984); *ibid.* **81**, 5533 (1984).
6. C. F. Wood, J. A. O'Neill, G. W. Flynn, *Chem. Phys. Lett.* **109**, 317 (1984).
7. J. A. O'Neill, J. Y. Cai, G. W. Flynn, R. E. Weston, Jr., *J. Chem. Phys.* **84**, 50 (1986).

8. J. A. O'Neill and G. W. Flynn, *Laser Focus* **1985**, 136 (June 1985); W. Jalenak, R. Weston, T. Sears, G. W. Flynn, *J. Chem. Phys.* **83**, 6049 (1985); G. W. Flynn and R. E. Weston, Jr., *Annu. Rev. Phys. Chem.* **37**, 551 (1986); B. B. Brady, G. B. Spector, L. Chia, G. W. Flynn, *J. Chem. Phys.* **86**, 3245 (1987).
9. J. A. O'Neill, J. Y. Cai, C. X. Wang, G. W. Flynn, R. E. Weston, Jr., *J. Chem. Phys.* **85**, 4195 (1986); *ibid.* **88**, 6240 (1988).
10. T. Kreutz, J. O'Neill, G. W. Flynn, *ibid.* **87**, 4598 (1987).
11. J. Hershberger, A. Hewitt, G. W. Flynn, R. Weston, Jr., *ibid.*, p. 1894.
12. R. E. Weston, Jr., and G. W. Flynn, *Radiochim. Acta* **43**, 110 (1987); T. G. Kreutz and G. W. Flynn, *AIP Conf. Proc.* **172**, 280 (1989);J. Hershberger, S. Hewitt, G. W. Flynn, R. E. Weston, Jr., *J. Chem. Phys.* **88**, 7243 (1988).
13. J. Hershberger, J. Chou, G. W. Flynn, R. E. Weston, Jr., *Chem. Phys. Lett.* **149**, 51 (1988).
14. W. Jalenak, R. E. Weston, Jr., T. Sears, G. W. Flynn, *J. Chem. Phys.* **89**, 2015 (1988); J. Y. Cai, C. X. Wang, S. H. Liu, J. O'Neill, G. W. Flynn, *Acta Opt. Sin.* **8**, 324 (1988); *Chin. J. Chem. Phys.* **1**, 188 (1988).
15. F. Khan, T. Kreutz, L. Zhu, G. W. Flynn, R. E. Weston, Jr., *J. Phys. Chem.* **92**, 6170 (1988).
16. T. G. Kreutz, F. A. Khan, G. W. Flynn, unpublished results; F. A. Khan, T. G. Kreutz, G. W. Flynn, R. E. Weston, Jr., unpublished results; T. G. Kreutz, F. A. Khan, G. W. Flynn, unpublished results.
17. S. A. Hewitt, J. Hershberger, J. Chou, G. W. Flynn, R. E. Weston, Jr., unpublished results.
18. F. A. Khan, T. G. Kreutz, G. W. Flynn, R. E. Weston, Jr., unpublished results.
19. W. F. Libby, *J. Am. Chem. Soc.* **69**, 2523 (1947).
20. G. C. Schatz, M. S. Fitzcharles, L. B. Harding, *Faraday Discuss. Chem. Soc.* **84**, 359 (1987).
21. A. Shultz, H. W. Cruse, R. N. Zare, *J. Chem. Phys.* **57**, 1354 (1972).
22. C. R. Quick and J. J. Tiee, *Chem. Phys. Lett.* **100**, 223 (1983); K. Kleinermanns and J. Wolfrum, *Laser Chem.* **2**, 339 (1983); *Chem. Phys. Lett.* **104**, 157 (1984); K. Kleinermanns, E. Linnebach, J. Wolfrum, *J. Phys. Chem.* **89**, 2525 (1985).
23. G. Hoffmann, D. Oh, Y. Chen, Y. M. Engel, C. Wittig, unpublished results.
24. Y. Chen, G. Hoffmann, D. Oh, C. Wittig, *Chem. Phys. Lett.* **159**, 426 (1989).
25. A. Jacobs, M. Wahl, R. Weller, J. Wolfrum, *ibid.* **158**, 161 (1989); J. Wolfrum, *Faraday Discuss. Chem. Soc.* **84**, 191 (1987).
26. J. K. Rice, Y. C. Chung, A. P. Baronavski, private communication.
27. S. Buelow, G. Radhakrishnan, J. Catanzarite, C. Wittig, *J. Chem. Phys.* **83**, 444 (1985); G. Radhakrishnan, S. Buelow, C. Wittig, *ibid.* **84**, 727 (1986); S. Buelow, G. Radhakrishnan, C. Wittig, *J. Phys. Chem.* **91**, 5409 (1987); S. Buelow *et al.*, *ibid.* **90**, 1015 (1986); C. Wittig, S. Sharpe, R. A. Beaudet, *Acc. Chem. Res.* **21**, 341 (1988).
28. J. Rice, G. Hoffman, C. Wittig, *J. Chem. Phys.* **88**, 2841 (1988).
29. C. Wittig, Y. M. Engel, R. D. Levine, *Chem. Phys. Lett.* **153**, 411 (1988).
30. N. F. Scherer, L. R. Khundkar, R. B. Bernstein, A. H. Zewail, *J. Chem. Phys.* **87**, 1451 (1987).
31. M. Mozurkewich, J. J. Lamb, S. W. Benson, *J. Phys. Chem.* **88**, 6435 (1984); D. M. Golden, *J. Chem. Phys.* **83**, 108 (1977); S. W. Benson, *Thermochemical Kinetics* (Wiley, New York, 1976).
32. G. C. Schatz and M. S. Fitzcharles, in *Selectivity in Chemical Reactions*, J. C. Whitehead, Ed. (Kluwer, Dordrecht, 1988), pp. 353–365.
33. F. A. Baiocchi, T. A. Dixon, C. H. Joyner, W. Klemperer, *J. Chem. Phys.* **74**, 6544 (1981).
34. R. S. Altman, M. D. Marshall, W. Klemperer, *ibid.* **77**, 4344 (1982).
35. S. Sharpe, Y. Zeng, R. A. Beaudet, C. Wittig, unpublished results.
36. I thank G. Schatz and C. Wittig for providing copies of their work prior to publication and for many stimulating discussions about the collision dynamics of the H + CO_2 system. I am indebted to R. Weston, T. Kreutz, J. Hershberger, F. Khan, S. Hewitt, J. Chou, L. Zhu, J. O'Neill, C. X. Wang, J. Y. Cai, J. Chu, C. Wood, and R. Quick for their many contributions and collaborations in the gathering and interpretation of inelastic scattering data. Collision dynamics studies in my laboratory have been generously supported by the Department of Energy, the National Science Foundation, and the Joint Services Electronics Program.

Parasitic Protozoa and Helminths: Biological and Immunological Challenges

ADEL A. F. MAHMOUD

Parasitic protozoans and helminths pose considerable medical as well as scientific challenges. Investigations of the complex and very different life cycles of these organisms, their adaptation to the obligate parasitic mode of life, and their ability to face the hostile host environment have resulted in many exciting discoveries. Invasion of host erythrocytes by plasmodial sporozoites and intact skin by schistosomal cercariae are outlined as examples of the elaborate mechanisms of parasitism. Isolation and characterization of single protective antigens or subunit vaccines from these two organisms are examined as models for vaccine development. Finally, developments in exploring gene regulation in protozoans and free and parasitic nematodes are briefly outlined.

PARASITIC PROTOZOANS AND HELMINTHS REPRESENT TWO major groups of infectious agents that are responsible for considerable morbidity and mortality in human and animal populations. These agents have a wide geographic distribution and, as multiple infections are common in endemic areas, the total number of infections in humans far exceeds the world population. The distribution of some of these infections is expanding because of the increased prevalence of immunosuppressive conditions such as malignancies, chemotherapeutic medications, and retroviral infections. Approximately 1 billion people are infected by ascaris; 600 million by malaria-causing plasmodia and 300 million each by schistosomes and filariae (*1*). While information on morbidity and mortality is less complete, it is estimated that malaria alone causes 1 million deaths among children yearly and that other infections such as schistosomiasis and filariasis cause chronic debilitating conditions that are associated with loss of productivity and reduced life-span. Parasitic protozoans such as *Pneumocystis carinii*, *Toxoplasma gondii*, and *Cryptosporidium* are emerging as major opportunistic infections in those infected with HIV or in those with other immunosuppressive conditions (*2*).

In spite of this enormous public health impact, a staggering contrast exists between our knowledge of protozoan and helminthic

---

The author is professor and chairman, Department of Medicine at Case Western Reserve University School of Medicine and University Hospitals, Cleveland, OH 44106.